Vol. 82 (1992) ACTA PHYSICA POLONICA A No 6

ELECTRONIC SPECTRA OF RADICAL CATIONS AND THEIR CORRELATION WITH PHOTOELECTRON SPECTRA. VI. A REINVESTIGATION OF TWO-, THREE-, AND FOUR-RING CONDENSED AROMATICS

Z.H. KHAN

Department of Physics, Jamia Millia Islamia, Jamia Nagar, New Delhi-110025, India

(Received June 6, 1992; in final form October 5, 1992)

Earlier interpretations of the electronic spectra of two-, three-, and four-ring condensed aromatic hydrocarbon radical cations are reexamined in the light of the UV photoelectron spectroscopic data for their neutral precursors and improved open-shell self-consistent field configuration interaction (SCF-CI) calculations. From the electronic transition energies for some 33 aromatic radical cations obtained from electronic absorption spectra (EAS) and those inferred from photoelectron spectra (PES), the following correlation is found between the two types of spectroscopies: $E_{\mathrm{EAS}} = (0.23 \pm 0.20) + (0.98 \pm 0.01) E_{\mathrm{PES}}$. The slope of this line is very close to unity which shows that the matrix shift on going from the solid phase (electronic spectrum) to the vapour phase (PE spectrum) is almost negligible and that there is no appreciable change in the geometry of the molecules on ionization.

PACS numbers: 33.20.–t, 33.60.–q, 31.20.–d

1. Introduction

In the previous papers of this series [1, 2], electronic spectra of a wide variety of polycyclic aromatic hydrocarbon radical cations were analyzed on the basis of UV photoelectron spectroscopic data for their neutral counterparts. This, however, did not include the simpler aromatic systems, viz. naphthalene, anthracene, tetracene, and their isomers whose study is very important for the completeness of this work as well as for finding a general correlation between the two spectroscopic techniques. Although the electronic spectroscopy of such molecular ions is fairly well understood and the assignment of most of their electronic bands is more or less confirmed, the availability of the ultraviolet PES data on such species [3] offers an additional useful source to reexamine their electronic spectra.

Apart from the several aromatic systems studied in this paper, a comprehensive work on electronic absorption spectra of tetracyclic aromatic monopositive ions in boric acid (BA) glass has already been published by the author [4]. On the other hand, spectra of naphthalene, anthracene and phenanthrene cations in the same matrix, though available in the literature [5], are generally of poor quality and are limited to the spectral region 220–650 nm. In view of this, the EA spectra of the above ionic species are remeasured in BA glass in the region 200–900 nm, thus encompassing all their ionic bands. The ionic spectra are analyzed on the basis of PE spectroscopic data and open-shell SCF calculations with limited configuration interaction. In the end, a correlation is given between the electronic transition energies for radical cations obtained from optical and PE spectroscopic data for a large number of condensed-ring aromatics.

2. Experimental

Naphthalene (puriss grade; Koch-Light, England), anthracene (LR grade; BDH, England), phenanthrene (unknown source), and boric acid (AR grade; Qualigens Fine, Bombay) were used without further purification. To start with, boric acid crystals were heated in a crucible to about 400°C in a temperature-controlled oven. As soon as the boric acid melted, a small amount of the hydrocarbon was added to the melt which was thoroughly mixed. The melt was sandwiched between two slightly preheated glass plates placed 1–2 mm apart which, after cooling to room temperature, formed a rigid glass. Radical cations of the hydrocarbons were produced by irradiating the hydrocarbon-doped glasses with a 120 W Osram high-pressure mercury lamp for five hours. A quartz lens was used to focus the UV light on a small area of the film. Optical absorption measurements in the spectral region 190–900 nm were made on a Perkin–Elmer 552 UV-VIS spectrophotometer.

3. Computational details

Two types of open-shell SCF methods are used for calculating the electronic transition energies and intensities of the aromatic hydrocarbon radical cations: (i) Longuet-Higgins and Pople (LHP) method [6], and (ii) Wasilewski method [7] which itself is based on the open-shell SCF method of Roothaan [8]. These methods are based on different approaches and thus they provide the possibility to assign the electronic bands with greater confidence.

The ground state configuration for an open-shell system with an odd number of π electrons can be written in the form

$$^2\Psi_G = |\Phi_1\overline{\Phi}_1 \ldots \Phi_k\overline{\Phi}_k \ldots \Phi_m|, \tag{1}$$

where the subscript k refers to a doubly-occupied MO and m stands for the singly-occupied MO. Also, the molecular orbitals Φ_k and $\overline{\Phi}_k$ represent the spin orbitals $\Phi_k\alpha$ and $\Phi_k\beta$, respectively. If the vacant orbitals are denoted by x, the different types of excited doublet configurations can be constructed from the π one-electron excitations which can be classified as follows:

(i) I: $k \rightarrow m$,

(ii) A : $m \rightarrow m+1$,

(iii) B_1 : $m \rightarrow x$ $(x > m+1)$, and

(iv) B_2, B_3 : $k \rightarrow x$.

The classifications A and B_1 in the above are essentially of the same type, but they have been placed in different categories due to certain interesting characteristics of the former (HOMO → LUMO) transition [9]. The excitation $k \rightarrow x$ gives rise to the states B_2 and B_3 that arise from two different orientations of the spins α and β, i.e. $(1/2)^{1/2}\,(\alpha\beta\alpha - \beta\alpha\alpha)$ and $(1/6)^{1/2}\,(2\alpha\alpha\beta - \alpha\beta\alpha - \beta\alpha\alpha)$, respectively. The excited doublet configurations for the open-shell system can thus be written as

$$
\begin{aligned}
{}^2\Psi_I &= |\Phi_1\overline{\Phi}_1 \ldots \Phi_k\overline{\Phi}_m \ldots \Phi_m|,\\
{}^2\Psi_A &= |\Phi_1\overline{\Phi}_1 \ldots \Phi_k\overline{\Phi}_k \ldots \Phi_{m+1}|,\\
{}^2\Psi_{B_1} &= |\Phi_1\overline{\Phi}_1 \ldots \Phi_k\overline{\Phi}_k \ldots \Phi_x|,\\
{}^2\Psi_{B_2} &= (1/2)^{1/2}\left\{|\Phi_1\overline{\Phi}_1 \ldots \Phi_k\overline{\Phi}_x \ldots \Phi_m| - |\Phi_1\overline{\Phi}_1 \ldots \overline{\Phi}_k\Phi_x \ldots \Phi_m|\right\},\\
{}^2\Psi_{B_3} &= (1/6)^{1/2}\left\{2|\Phi_1\overline{\Phi}_1 \ldots \Phi_k\Phi_x \ldots \overline{\Phi}_m| - |\Phi_1\overline{\Phi}_1 \ldots \Phi_k\overline{\Phi}_x \ldots \Phi_m|\right.\\
&\quad \left. -|\Phi_1\overline{\Phi}_1 \ldots \overline{\Phi}_x\Phi_x \ldots \Phi_m|\right\}. \qquad (2)
\end{aligned}
$$

Formulas for CI matrix elements between different configurations (ground as well as excited) in the framework of the LHP method are given by Carsky and Zahradnik [10]. For the other method, the corrected version of formulas given by Wasilewski [7] were used which also involve the open-shell $\mathcal{J}$ matrix over MOs whose elements are:

$$
\begin{aligned}
\mathcal{J}_{kl} &= F_{kl} + [kl|mm] + 1/2[km|lm],\\
\mathcal{J}_{km} &= F_{km} + [km|mm],\\
\mathcal{J}_{kx} &= F_{kx} + [kx|mm] - 1/2[km|mx],\\
\mathcal{J}_{mm} &= F_{mm} + 1/2[mm|mm],\\
\mathcal{J}_{mx} &= F_{mx},\\
\mathcal{J}_{xy} &= F_{xy} + [mm|xy] - 3/2[mx|my]. \qquad (3)
\end{aligned}
$$

In these formulas, F_{ij} represent the elements of the closed-shell F matrix over MOs which can be expressed as

$$F_{ij} = H_{ij}^{\text{core}} + \sum_k \left(2[ij|kk] - [ik|jk]\right), \qquad (4)$$

where H_{ij}^{core} are matrix elements of the core Hamiltonian. Using the LCAO MO approximation, the matrix elements F_{ij} can be written in terms of the elements of the closed-shell F matrix over AOs $F_{\mu\nu}$, viz.

$$F_{ij} = \sum_{\mu} c_{i\mu} c_{j\mu} F_{\mu\mu} + \sum_{\mu} \sum_{\mu \neq \nu} \sum_{\nu} c_{i\mu} c_{j\nu} F_{\mu\nu}. \tag{5}$$

Expression (5) involves the F matrix over AOs $F_{\mu\nu}$, which are evaluated using the Pariser–Parr method [12] according to which

$$F_{\mu\mu} = -I_{\mu} + 1/2 P_{\mu\mu} \gamma_{\mu\mu} + \sum_{\nu \neq \mu} (P_{\nu\nu} - z_{\nu}) \Gamma_{\mu\nu}, \tag{6}$$

$$F_{\mu\nu} = \beta_{\mu\nu} - 1/2 P_{\mu\nu} \Gamma_{\mu\nu}, \quad \text{for } \mu \neq \nu, \tag{7}$$

where I_{μ} is the ionization energy of the atom μ, z_{ν} is the charge on the atom ν in the core, $\beta_{\mu\nu}$ are the elements of the resonance integral, $\Gamma_{\mu\nu}$ are the Coulomb repulsion integrals, and $P_{\mu\nu}$ are the elements of the density matrix defined by

$$P_{\mu\nu} = \begin{cases} 2 \sum_k c_{k\mu} c_{k\nu} + c_{m\mu} c_{m\nu} & \text{(for LHP method)}, \\ 2 \sum_k c_{k\mu} c_{k\nu} & \text{(for Wasilewski method)}. \end{cases} \tag{8}$$

The resonance integrals $\beta_{\mu\nu}$ are chosen as -2.318 eV if the atoms μ and ν are bonded and taken as zero when they are not bonded. The electron interaction integrals $[ij|rs]$ are expressed as

$$[ij|rs] = \sum_{\mu} \sum_{\nu} c_{i\mu} c_{j\mu} c_{r\nu} c_{s\nu} \Gamma_{\mu\nu}. \tag{9}$$

The one-centre Coulomb integrals $\Gamma_{\mu\mu}$ are taken as the difference of the ionization potential I_{μ} and electron affinity A_{μ} for the respective atoms,

$$\Gamma_{\mu\mu} = I_{\mu} - A_{\mu}. \tag{10}$$

Choosing $I_{\mu} = 11.22$ eV and $A_{\mu} = 0.69$ eV for carbon sp^2 valence state, we obtain, $\Gamma_{\mu\mu} = 10.53$ eV. The two-centre integrals $\Gamma_{\mu\nu}$ were evaluated using the Mataga–Nishimoto approximation [13],

$$\Gamma_{\mu\nu} = 14.3986 / \{R_{\mu\nu} + 14.3986 / [0.5(\Gamma_{\mu\mu} + \Gamma_{\nu\nu})]\}, \tag{11}$$

where $R_{\mu\nu}$ is the interatomic distance which is chosen as a constant (1.4 Å) for all the C–C bonds in the molecular systems under investigation.

Based on the above formulations, a computer programme was written which automatically selects the configurations with certain energy cut-off such that their number does not exceed the maximum limit of configurations as defined in the programme. In the present case, this number was chosen as 62. Finally, the energies of electronic transitions, their transition moments and oscillator strengths were calculated. All the calculations were made on a Cyber 170 Computer at the National Informatics Centre, New Delhi.

4. Results and discussion

In the following figures we have sketched the electronic absorption spectra for radical cations of naphthalene, anthracene, tetracene and their isomers. At the top of each figure, electronic transition energies for cations inferred from the ultraviolet PE spectra of their neutral precursors are shown as vertical lines. These energies are obtained from the difference between the $(n+1)$-th and first ionization potentials (IPs) of the corresponding parent molecules:

$$E_n = IP_{n+1} - IP_1 \quad (n \geq 1), \tag{12}$$

where E_n refers to the energy of the n-th electronic transition of a radical cation. In the lower half of the figures, calculated electronic transition energies for cations along with their oscillator strengths are shown as stick diagrams where lengths of the sticks indicate their relative oscillator strengths. Forbidden transitions are shown by dotted vertical lines which, in most of the cases, are shown only for the lower-energy region to avoid overcrowding of calculated spectra.

A close look at the calculated electronic transitions for the ions reveals that the results of open-shell SCF-CI calculations based on the LHP and Wasilewski methods show a great resemblance, especially for the lower-energy region. In view of this, we have generally adopted the Wasilewski method for interpretation of the optical spectra. However, in cases where there is some ambiguity in the assignments, help is also taken from LHP calculations. A detailed discussion for each of the molecular ions is given in the following.

4.1. Naphthalene cation

Figure 1 displays a complete picture of the electronic absorption spectrum of naphthalene cation in BA glass together with the calculated spectrum and energies for several electronic transitions for the cation obtained from the PE spectrum of the neutral molecule. The EA spectrum in BA glass greatly resembles the spectrum of the species reported by Shida and Iwata [14] which were produced in the glassy matrices of sec-butyl chloride and freon mixture at 77 K by gamma irradiation. The present spectrum has two additional absorption bands at 36.1 and 45.0 kK that do not appear in the spectrum measured by the above workers.

The electronic absorption spectrum of naphthalene shows six major absorption band systems at 14.7, 21.4, 26.1, 32.2, 36.1, and 45.0 kK which agree with the measurements of Andrews et al. [15]. More recently, Salama and Allamandola [16] have reported highly resolved EA spectra of naphthalene cation in argon and neon matrices at 4.2 K which contain all the absorption bands measured in the boric acid matrix. To understand the origin of these bands, we reproduce in the following the prominent configurations for those doublet excited states of the cation which are relevant to the observed spectrum. These, in the light of Wasilewski calculations are:

(1) I [$0.96(4 \rightarrow 5)$], 8.1 (0.000);
(2) I [$-0.95(3 \rightarrow 5)$], 14.5 (0.092);
(3) IA [$0.76(2 \rightarrow 5) - 0.58(5 \rightarrow 6)$], 19.6 (0.005);
(4) AB_3 [$-0.66(5 \rightarrow 6) + 0.45(4 \rightarrow 7) - 0.45(2 \rightarrow 5)$], 22.8 (0.113);

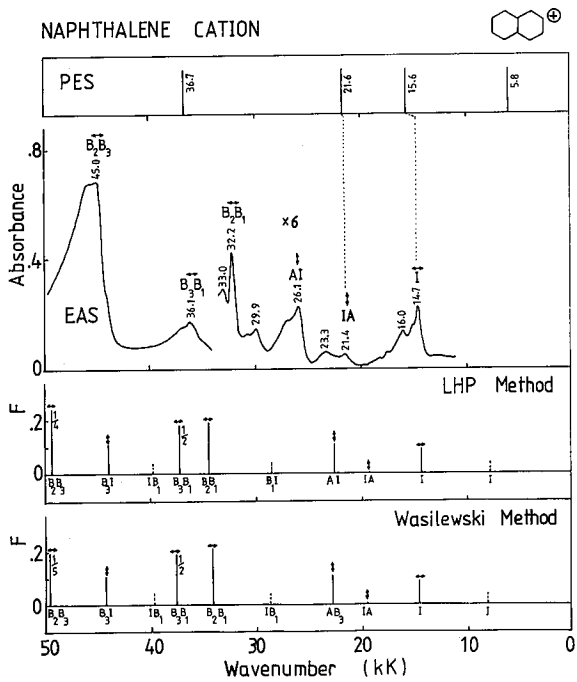

Fig. 1. Electronic absorption spectrum (EAS) of naphthalene cation and its comparison with the calculated spectrum and the transition energies estimated from the UV photoelectron spectrum (PES) of the parent molecule. In the EA spectrum, calculated polarizations of individual electronic bands are also given. The dotted vertical lines in the calculated spectra correspond to forbidden transitions and the "fractions" show the amount by which the actual oscillator strengths have been reduced in the diagram.

(5) B_2B_1 $[-0.72(4 \rightarrow 6) - 0.54(5 \rightarrow 7) - 0.39(4 \rightarrow 6)]$, 34.2 (0.207);
(6) B_3B_1 $[0.66(4 \rightarrow 6) - 0.66(5 \rightarrow 7)]$, 37.8 (0.373);
(7) B_2B_3 $[-0.65(4 \rightarrow 6) + 0.57(4 \rightarrow 6) + 0.45(5 \rightarrow 7)]$, 49.6 (0.959).
Here, the symbols on the left represent the class to which the electronic transitions belong. One-letter symbols are used for *pure* one-electron excitations where the contribution from each of the remaining configurations has a value less than 0.3. Two-letter symbols are used for such cases for which the second or higher configuration also has appreciable contribution. To differentiate such transitions from the *pure* ones, we call them as *mixed*. In some cases, even the third configuration has a significant contribution, but this has not been used in the classification simply to avoid further complexity. The coefficients of state functions are given in brackets followed by the electronic configurations. The two figures on the extreme right correspond to the calculated electronic transition energies and their oscillator strengths, the latter being written within parentheses.

In the ultraviolet PE spectrum of naphthalene molecule, five π electron peaks have been identified [3] from which we obtain energies for four electronic transitions

for its cation. The first line which is optically forbidden, is not accessible in the present measurement, but it appears in the PES diagram in the near IR region (5.8 kK). It arises due to the one-electron excitation $\Phi_4 \rightarrow \Phi_5$. The next I transition arising from the excitation $\Phi_3 \rightarrow \Phi_5$, is observed in the optical spectrum at 14.7 kK. It corresponds to the second PES line at 15.6 kK. The PE spectrum of naphthalene, as reported by Dewar et al. [17], gives the location of the second PES line at 14.8 kK which is very close to the value obtained from the optical spectrum. The next two transitions result from the mixing between the configurations $\Phi_2 \rightarrow \Phi_5$ and $\Phi_5 \rightarrow \Phi_6$ with most of the intensity confined in the latter. The third PES line at 21.6 kK shows an excellent agreement with the 21.4 kK weak absorption and is assigned as the y-polarized IA transition. The absorption band at 26.1 kK can be classified as AB_3 in the light of Wasilewski calculations, whereas the LHP method designates it as AI. We have adopted the latter assignment as it is also favoured by other workers [14]. This band has the dominant non-Koopmans character and it does not appear in the PES diagram. It might be mentioned that both of the theories underestimate the energies of the IA and AI bands. The absorption bands at 32.2, 36.1, and 45.0 kK are strong in intensity and are polarized along the x-axis of the molecule. On the basis of the calculations, these are classified as the B_2B_1, B_3B_1, and B_2B_3, respectively. The fourth PES line at 36.7 kK is optically forbidden and could not be detected in the EA spectrum.

4.2. Anthracene cation

In view of the importance of lower-energy electronic transitions characterizing ionic species, the prominent configurations for some of the doublet states of anthracene cation are listed below:

(1) I [$-0.96(5 \rightarrow 7)$], 13.2 (0.000);
(2) I [$-0.96(6 \rightarrow 7)$], 14.3 (0.166);
(3) AI [$0.88(7 \rightarrow 8) - 0.34(4 \rightarrow 7)$], 15.4 (0.027);
(4) IB_3 [$0.80(4 \rightarrow 7) - 0.40(5 \rightarrow 9)$], 23.6 (0.115);
(5) B_2B_1 [$0.69(5 \rightarrow 8) + 0.53(7 \rightarrow 9) + 0.41(5 \rightarrow 8)$], 30.4 (0.247);
(6) B_1B_3 [$-0.66(7 \rightarrow 9) + 0.62(5 \rightarrow 8)$], 35.1 (0.616);
(7) B_2B_1 [$-0.56(5 \rightarrow 8) + 0.47(7 \rightarrow 9) + 0.40(5 \rightarrow 8)$], 43.8 (1.407).

In all of them six π photoelectron peaks have been identified in the PE spectrum of anthracene [3] from which we obtain the energies for five electronic transitions for its radical cation as shown at the top of Fig. 2. The first PES line at 9.1 kK is optically forbidden and it does not appear in the EA spectrum. Hiratsuka et al. [18] have, however, observed a weak absorption in the lower-energy region of the electronic spectrum of naphthalene cation in stretched polymer films and assigned it as y-polarized on the basis of their polarization measurements. Present results based on the PES data as well as theoretical calculations do not support the assignment given by the above workers which is also in agreement with the interpretation given by Shida et al. [14]. The 14.0 kK absorption band well corresponds to the second PES line at 14.4 kK. It arises from the pure one-electron excitation, $\Phi_6 \rightarrow \Phi_7$. The next transition, arising from the interaction between the configurations $\Phi_7 \rightarrow \Phi_8$ and $\Phi_4 \rightarrow \Phi_7$, is of AI type. It has the dominant

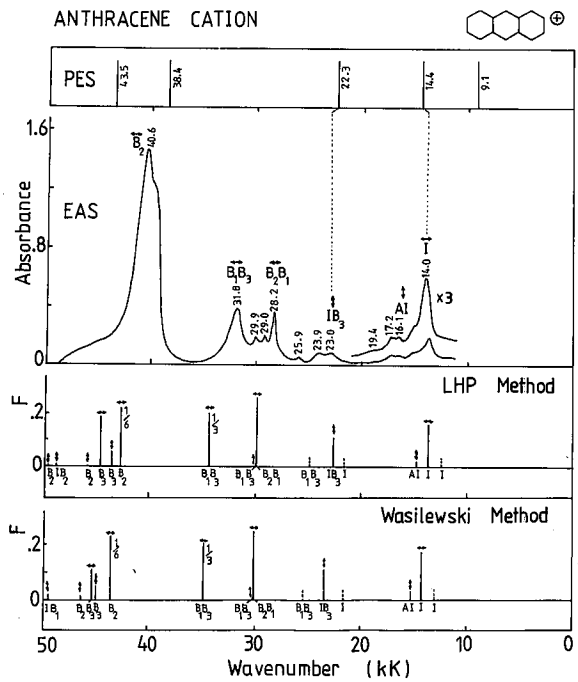

Fig. 2. Electronic absorption spectrum of anthracene cation and its comparison with the calculated spectrum and the transition energies estimated from the UV photoelectron spectrum of the molecule. For other details, see caption to Fig. 1.

non-Koopmans character and does not show up in the PES diagram; but it does appear as a weak band at 16.1 kK in the EA spectrum. In this we differ from the assignment made by Spanget-Larsen [19] who considers the weak absorption at 19.4 kK as the *AI* transition. Our assignment is further confirmed from the polarization measurements of anthracene cation by Hiratsuka et al. [18] and with the cation spectrum in argon matrix by Bally [20]. The third PES line shows good agreement with the 23.0 kK electronic band. It arises due to mixing between the configurations $\Phi_4 \rightarrow \Phi_7$ and $\Phi_5 \rightarrow \Phi_9$. The higher-energy electronic absorption bands of anthracene cation are easily assigned on the basis of the calculated transition energies and their intensities.

4.3. Phenanthrene cation

From the PE spectrum of phenanthrene molecule, four electronic transitions for its cation are obtained as shown in Fig. 3. These can be well explained on the basis of the calculated excited state configurations for the cation as given in the following:

(1) I [$-0.95(6 \rightarrow 7)$], 5.4 (0.008);
(2) I [$-0.93(5 \rightarrow 7)$], 12.3 (0.101);

(3) I [0.90(4 → 7)], 16.9 (0.000);
(4) I [−0.88(3 → 7)], 19.9 (0.065);
(5) AB_3 [−0.82(7 → 8) − 0.37(6 → 9)], 22.4 (0.179);
(6) I [0.72(2 → 7)], 26.3 (0.031).

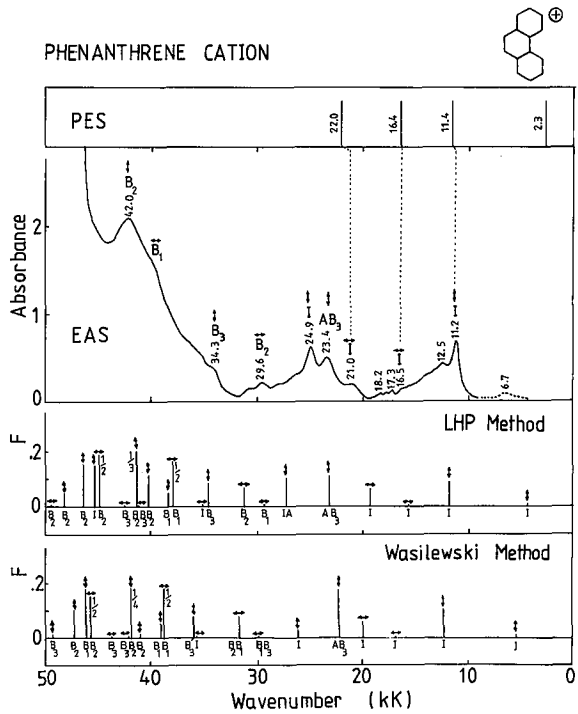

Fig. 3. Electronic absorption spectrum of phenanthrene cation and its comparison with the calculated spectrum and the transition energies estimated from the UV photoelectron spectrum of the molecule. For other details, see caption to Fig. 1.

The calculations predict a weak transition which fits the first PES line at 2.3 kK. This transition could not be observed in the present experiment due to limitations of the apparatus used. Shida and Iwata [14] have, however, noticed an absorption band at 6.7 kK which shows a considerable shift from the first PES line. The second absorption at 11.2 kK matches with the 11.4 kK PES line. The third and fourth transitions appear as weak bands at 16.5 and 21.0 kK which correspond to the third and fourth PES lines at 16.4 and 22.0 kK, respectively. In the absorption spectrum reported by Zaidi and Khanna [5], no optical bands with energies less than 21 kK were observed. The next absorption band at 23.4 kK (AB_3) arises due to interaction between the configurations $\Phi_7 \rightarrow \Phi_8$ and $\Phi_6 \rightarrow \Phi_9$ and has a predominant non-Koopmans character. The absorption at 24.9 kK is of I type ($\Phi_2 \rightarrow \Phi_7$). Its intensity is underestimated by Wasilewski calculations, but the LHP method gives a better estimate of the intensity. This transition is absent

in the PES diagram as the identification of the fifth and higher-energy π bands in the PE spectrum of phenanthrene is difficult to make due to σ ionization in the higher-energy region.

4.4. Tetracene cation

Although a detailed spectroscopic study of tetracene radical cation has already been made by the author [4] and the assignment of various electronic bands is almost well settled, there is still some confusion about the location of the weak *A* type electronic band in the optical spectrum. To resolve this problem and to get a better understanding of the overall optical spectrum, we reproduce in the following some of the important excited state configurations calculated in the framework of the Wasilewski method:

(1) *I* [0.94(8 → 9)], 12.2 (0.261);

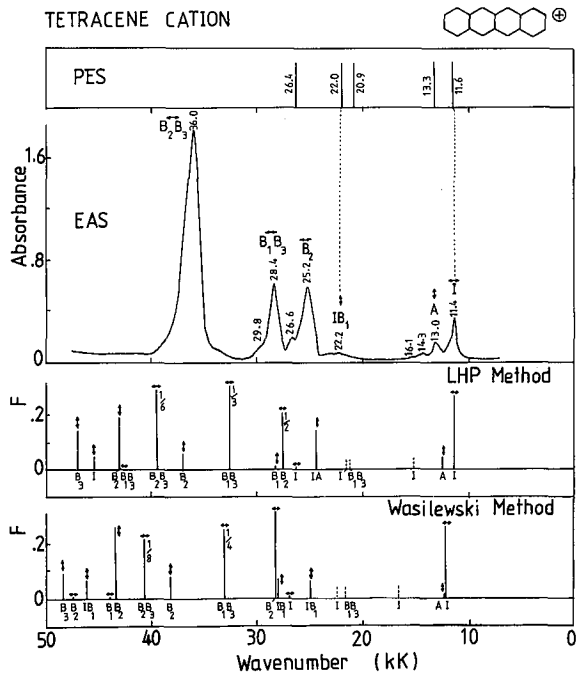

Fig. 4. Electronic absorption spectrum of tetracene cation and its comparison with the calculated spectrum and the transition energies estimated from the UV photoelectron spectrum of the molecule. For other details, see caption to Fig. 1.

(2) *A* [−0.91(9 → 10)], 12.3 (0.045);
(3) *I* [0.93(7 → 9)], 16.7 (0.000);
(4) *I* [−0.93(5 → 9)], 22.5 (0.000);
(5) IB_1 [−0.59(6 → 9) − 0.43(9 → 13)], 25.0 (0.057);
(6) IB_1 [0.66(6 → 9) − 0.47(9 → 13)], 28.2 (0.073);

(7) B_2B_1 [$-0.68(7 \rightarrow 10) - 0.48(9 \rightarrow 12) - 0.44(7 \rightarrow 10)$], 28.2 (0.316);
(8) B_1B_3 [$-0.72(9 \rightarrow 12) + 0.55(7 \rightarrow 10)$], 33.4 (1.039);
(9) B_2B_3 [$-0.61(7 \rightarrow 10) + 0.55(7 \rightarrow 10) + 0.38(9 \rightarrow 12)$], 40.7 (1.731).

From the PE spectrum of tetracene molecule, we infer five electronic transitions for the cation as shown in the PES diagram (Fig. 4). The first PES line shows perfect agreement with the 11.4 kK band in the EA spectrum and that predicted by the calculations. The next transition (A type) is presumably hidden in the vibrational structure of the 13.0 kK optical band. The PES line at 13.3 kK corresponds to the third I type electronic transition which is symmetry-forbidden. The next I type electronic transition is also optically forbidden which does not show up in the EA spectrum, but its location is correctly predicted by the calculations. It, however, appears as the third line in the PES diagram. The fourth PES line exactly corresponds to the weak absorption at 22.2 kK and is assigned as IB_1. According to Wasilewski calculations, the next line in the PES diagram is identified as the IB_1 transition resulted due to interaction between the configurations $\Phi_6 \rightarrow \Phi_9$ and $\Phi_9 \rightarrow \Phi_{13}$, but it is not observed in the absorption spectrum owing to its poor intensity. The three strong absorption bands at 25.2, 28.4, and 36.0 kK are easily identified as the x-polarized transitions B_2, B_1B_3, and B_2B_3, respectively.

4.5. 1.2-Benzanthracene cation

In the PE spectrum of neutral 1.2-benzanthracene molecule [3], six π bands have been identified from which the energies for the five lower-energy electronic transitions of the radical cation are obtained as depicted at the top of Fig. 5. These can be explained on the basis of the following lower-energy excited states of the cation calculated by using the Wasilewski method:
(1) I [$0.92(8 \rightarrow 9)$], 7.4 (0.044);
(2) I [$-0.91(7 \rightarrow 9)$], 13.5 (0.155);
(3) IA [$-0.77(6 \rightarrow 9) + 0.50(9 \rightarrow 10)$], 17.2 (0.002);
(4) IA [$0.56(5 \rightarrow 9) + 0.56(9 \rightarrow 10) + 0.41(6 \rightarrow 9)$], 19.3 (0.049);
(5) IA [$0.58(5 \rightarrow 9) - 0.47(4 \rightarrow 9) - 0.37(9 \rightarrow 10)$], 21.7 (0.071);
(6) I [$-0.72(4 \rightarrow 9)$], 24.3 (0.122);
(7) B_2B_1 [$0.58(8 \rightarrow 10) + 0.41(9 \rightarrow 11)$], 28.9 (0.224).

The first PES line located at 5.1 kK is well predicted from the calculations, but it could not be detected due to limitations of the present experiment. This band has been observed by Shida and Iwata [14] at 5.4 kK in the absorption spectrum of the cation in sec-butyl chloride. The next absorption band at 11.2 kK is strong in intensity and shows a good correspondence with the second PES line at 11.7 kK. Both of these transitions are pure one-electron excitations, while the remaining transitions have generally mixed character. The third electronic transition (IA type), arising due to the mixing between the configurations $\Phi_6 \rightarrow \Phi_9$ and $\Phi_9 \rightarrow \Phi_{10}$, is observed at 15.3 kK and matches with the 15.9 kK line in the PES diagram. The Wasilewski method overestimates the Koopmans nature of the 17.6 kK transition which has comparable contributions from $\Phi_9 \rightarrow \Phi_{10}$ and $\Phi_5 \rightarrow \Phi_9$ excitations, whereas the LHP method reveals its true non-Koopmans

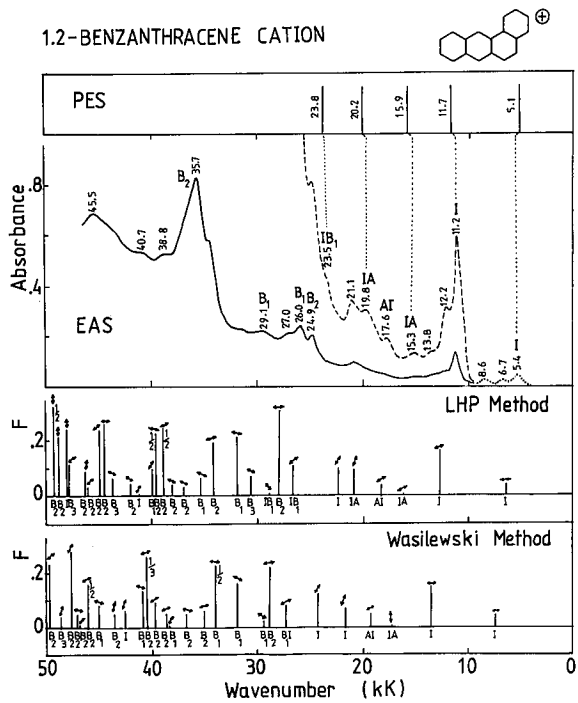

Fig. 5. Electronic absorption spectrum of 1.2-benzanthracene cation and its comparison with the calculated spectrum and the transition energies estimated from the UV photoelectron spectrum of the molecule. In the EA spectrum, the solid and dashed curves correspond to the low and high solute concentrations, respectively; the dotted curve is reproduced from Ref. [14]. For other details, see caption to Fig. 1.

nature. In the light of this, the 17.6 kK band is assigned as AI. In our earlier paper [4], the absorption at 19.8 kK was wrongly attributed to the AI transition. In fact, the 19.8 kK band (with a vibrational structure at 21.1 kK) arises due to the interaction among the configurations $\Phi_5 \rightarrow \Phi_9$, $\Phi_4 \rightarrow \Phi_9$, and $\Phi_9 \rightarrow \Phi_{10}$. The absorption band located at 23.5 kK in the EA spectrum is a pure one-electron excitation $\Phi_4 \rightarrow \Phi_9$ and corresponds to the 23.8 kK line in the PES diagram. The next absorption at 24.9 kK is assigned as B_2. The identification of absorption bands above 25 kK is difficult to make owing to the overcrowding of calculated spectral lines. In some cases, however, a tentative assignment of electronic bands is possible on the basis of the calculations.

4.6. Chrysene cation

Experimental and theoretical results for the transition energies of chrysene radical cation are depicted in Fig. 6. The lower-energy excited states along with their prominent configurations are as follows:
(1) I [$-0.96(7 \rightarrow 9)$], 7.4 (0.000);

(2) I [0.95(8 → 9)], 9.6 (0.184);
(3) I [0.90(6 → 9)], 17.5 (0.006);
(4) I [0.94(5 → 9)], 18.6 (0.000);
(5) IA [−0.74(4 → 9) + 0.54(9 → 10)], 21.6 (0.106);
(6) AI [0.68(9 → 10) + 0.50(4 → 9) + 0.32(8 → 12)], 24.6 (0.315);
(7) B_2B_3 [−0.52(7 → 10) − 0.44(7 → 10) − 0.36(9 → 13)], 30.2 (0.149);
(8) B_3B_1 [−0.52(7 → 10) − 0.48(9 → 11) + 0.32(2 → 9)], 35.5 (0.477).

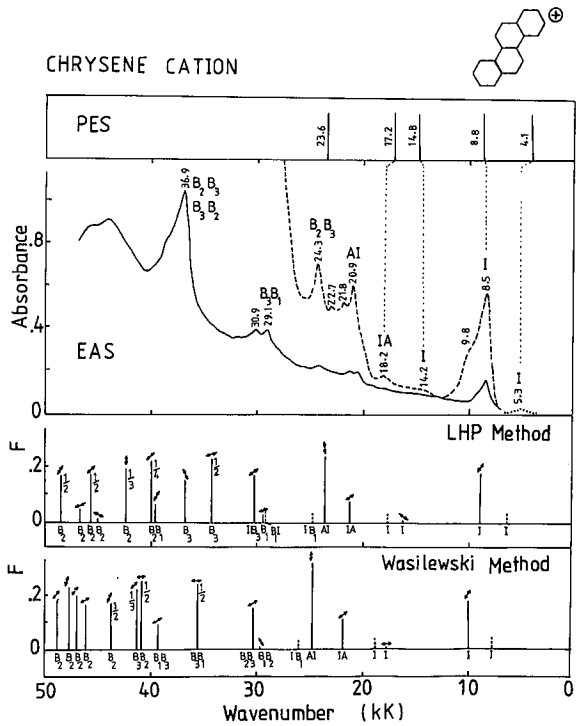

Fig. 6. Electronic absorption spectrum of chrysene cation and its comparison with the calculated spectrum and the transition energies estimated from the UV photoelectron spectrum of the molecule. For other details, see captions to Figs. 1 and 5.

From the above, it is obvious that the first four electronic transitions are I type "pure" one-electron excitations out of which only the second ($\Phi_8 \rightarrow \Phi_9$) and the third ($\Phi_6 \rightarrow \Phi_9$) ones are allowed and have been observed in the optical spectrum at 8.5 and 14.2 kK, respectively. These bands show an excellent correspondence with the second and third PES lines at 8.8 and 14.8 kK, respectively. In our earlier paper [4], the band at 14.2 kK could not be assigned due to the shortcoming of the theoretical method used for calculations. The first and fourth electronic transitions are symmetry-forbidden, but they do appear in the PES diagram. In the spectrum of the cation in sec-butyl chloride measured by Shida and Iwata [14], a weak absorption band is noticed at 5.3 kK which, due to its

proximity to the first PES line at 4.1 kK, seems to be the first I type transition. The fifth (IA) and sixth (AI) electronic transitions result due to the mixing of the configurations $\Phi_4 \rightarrow \Phi_9$ and $\Phi_9 \rightarrow \Phi_{10}$ with most of the intensity confined in the latter. In view of the fact that only the I type transitions with the dominant Koopmans character are allowed in the PE spectrum, we assign the 18.2 kK band as the IA transition which corresponds to the 17.2 kK PES line. The absorption at 20.9 kK has no match in the PES diagram and is assigned as the non-Koopmans type AI transition. This band shows structures at 21.8 and 22.7 kK with a vibrational frequency of $\approx$ 900 cm^{-1}. The next electronic transition IB_1, which is symmetry-forbidden, is not observed in the EA spectrum, but it appears as the fifth line in the PES diagram. The optical band at 24.3 kK belongs to the class B_2B_3 whose Koopmans character is overestimated by the LHP method. It might be mentioned that both of the theoretical methods overestimate the energies of all transitions above 20 kK. In view of this, the 29.1 kK band is assigned as the B_3B_1 transition. Identification of absorption bands above 30 kK is rather complicated as the calculations predict too many electronic transitions in this region. It is, therefore, difficult to identify the exact nature (B_2B_3 or B_3B_2) of the 36.9 kK band.

4.7. 3.4-Benzphenanthrene cation

Observed and calculated spectra of 3.4-benzphenanthrene cation are plotted in Fig. 7. The origin of the electronic transitions can be easily understood from the configurations of the excited states listed below:

(1) I [0.96(8 → 9)], 3.0 (0.013)
(2) I [−0.93(7 → 9)], 10.6 (0.146)
(3) I [−0.97(6 → 9)], 13.3 (0.014);
(4) I [−0.94(4 → 9)], 19.5 (0.046);
(5) I [0.90(5 → 9)], 19.7 (0.004);
(6) AI [0.76(9 → 10) − 0.38(3 → 9) − 0.38(8 → 11)], 22.8 (0.027);
(7) B_1I [−0.54(9 → 12) − 0.40(2 → 9) + 0.34(9 → 11)], 27.2 (0.003);
(8) IA [0.78(3 → 9) + 0.32(9 → 10)], 28.1 (0.028);
(9) B_2B_1 [0.65(8 → 10) + 0.55(9 → 11)], 29.5 (0.114);
(10) B_3B_1 [−0.54(8 → 10) + 0.45(9 → 11)], 31.9 (0.617);
(11) B_2 [0.76(8 → 11)], 38.4 (0.643).

At the top of Fig. 7, the energies for the first five electronic transitions for 3.4-benzphenanthrene radical cation are depicted as estimated from the PE spectrum of the parent molecule. The first line in the PES diagram located at 3.4 kK is correctly predicted by the calculations, but it could not be accessible due to experimental limitations. The strong absorption band at 10.6 kK shows good agreement with the 11.1 kK PES line and it is assigned as the I type transition $\Phi_7 \rightarrow \Phi_9$. The next electronic transition $\Phi_6 \rightarrow \Phi_9$, which is also of I type, is weak in intensity and overlaps with the vibrational structure of the 10.6 kK band. On the basis of the PE spectrum, the energy of this band is estimated as 12.7 kK. The fourth and fifth electronic transitions are also pure one-electron excitations, $\Phi_4 \rightarrow \Phi_9$ and $\Phi_5 \rightarrow \Phi_9$, respectively. These are predicted to be within close proximity, but are well separated in the optical spectrum and are located at 18.5 and

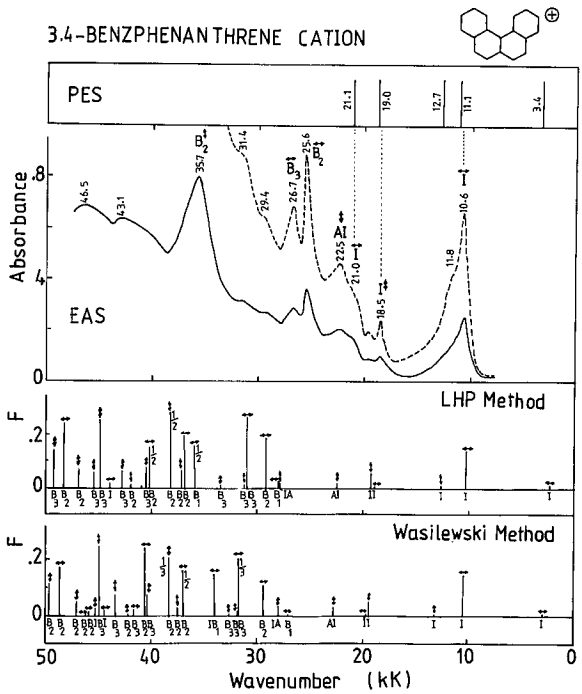

Fig. 7. Electronic absorption spectrum of 3.4-benzphenanthrene cation and its comparison with the calculated spectrum and the transition energies estimated from the UV photoelectron spectrum of the molecule. For other details, see caption to Fig. 1.

21.0 kK, respectively. These transitions correspond to the fourth and fifth lines in the PES diagram. The sixth and eighth transitions are of mixed character and arise due to the interaction between the configurations $\Phi_9 \rightarrow \Phi_{10}$ and $\Phi_3 \rightarrow \Phi_9$. The lower-energy component (AI) of the transition resulted from this mixing is located in the optical spectrum at 22.5 kK. The theoretical spectrum beyond 25 kK is rather too complex because of overcrowding. However, the intensity considerations make possible a tentative assignment of the absorption bands at 25.6, 26.7 and 35.7 kK as $B_2(x)$, $B_3(x)$ and $B_2(y)$, respectively.

4.8. Triphenylene cation

Figure 8 sketches the observed and calculated electronic spectra of triphenylene cation that are simple enough to facilitate the assignment of the individual optical bands. The important lower-energy excited states of the cation, together with the major configurations, are:

(1) I [0.98(8 → 9)], 1.3 (0.000);
(2) I [0.96(7 → 9)], 6.7 (0.050);
(3) I [0.85(4 → 9) − 0.42(6 → 9)], 14.9 (0.090);
(4) I [0.95(5 → 9)], 15.3 (0.047);

(5) I [$0.84(6 \rightarrow 9) + 0.41(4 \rightarrow 9)$], 17.0 (0.105);
(6) IA [$0.59(2 \rightarrow 9) - 0.43(9 \rightarrow 10) - 0.39(7 \rightarrow 12)$], 26.5 (0.025);
(7) AI [$0.63(9 \rightarrow 10) + 0.54(2 \rightarrow 9) + 0.38(8 \rightarrow 11)$], 29.9 (0.028).

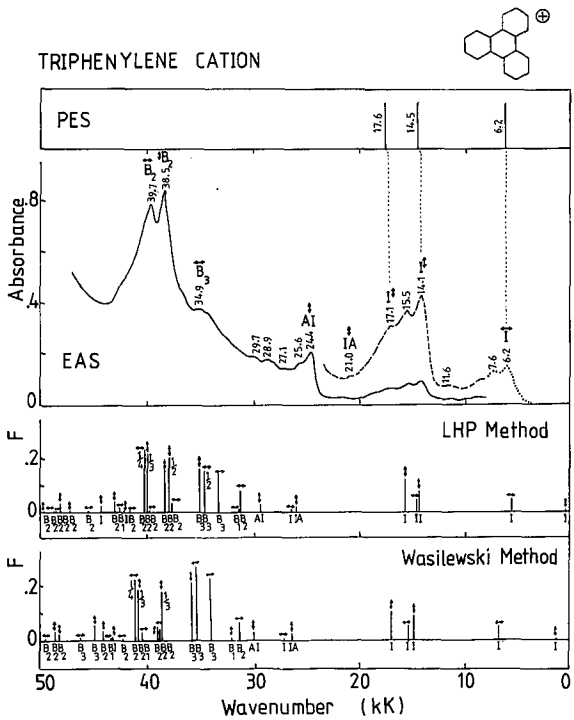

Fig. 8. Electronic absorption spectrum of triphenylene cation and its comparison with the calculated spectrum and the transition energies estimated from the UV photoelectron spectrum of the molecule. For other details, see captions to Figs. 1 and 5.

The first electronic transition of the cation as predicted to be located in the near IR region, does not appear in the PES diagram. This is due to the fact that triphenylene has a degenerate ground state for which the theory employed in this work is rather inadequate. Due to experimental limitations, the first allowed transition could not be measured in BA glass. However, Shida and Iwata [14] have reported an absorption at 6.2 kK of triphenylene cation produced in sec-butyl chloride by gamma irradiation at 77 K which exactly matches with the first line in the PES diagram and is assigned as the x-polarized I transition $\Phi_7 \rightarrow \Phi_9$. The third and fifth electronic transitions result from the mixing between the configurations $\Phi_4 \rightarrow \Phi_9$ and $\Phi_6 \rightarrow \Phi_9$. These transitions correspond to the PES lines at 14.5 and 17.6 kK and are observed in the EA spectrum at 14.1 and 17.1 kK, respectively. The fourth transition is a pure one-electron excitation $\Phi_5 \rightarrow \Phi_9$ and lies within close proximity to the third I transition and is not observed in the optical spectrum. The mixing of the configurations $\Phi_2 \rightarrow \Phi_9$ and $\Phi_9 \rightarrow \Phi_{10}$ gives rise to the transitions IA

and *AI*. These are identified in the optical spectrum as the weak and strong bands located at 21.0 and 24.4 kK, respectively. In contrast to experimental findings, both calculations predict the intensity of the latter electronic band to be too weak. This disagreement is generally attributed to Jahn–Teller distortion. Once again, the calculations predict too many electronic transitions in the higher-energy region making the identification of the individual absorption bands rather difficult. In view of this, only a tentative assignment for the higher-energy bands is possible.

4.9. Correlation between "I" type electronic transitions for cations obtained from optical absorption and photoelectron spectra

Fitting the experimental data for the "*I*" type electronic transition energies obtained from electronic absorption spectra of radical cations for some 33 aromatic hydrocarbons studied by the author in this and the previous papers of the series [1, 2] with those estimated from the PE spectra of their neutral precursors, the following correlation is obtained (Student's t-test, 116 degrees of freedom):

$$E_{\mathrm{EAS}} = (0.23 \pm 0.20) + (0.98 \pm 0.01) E_{\mathrm{PES}}, \tag{13}$$

$$SE(E_{\mathrm{EAS}}) = 0.68 \text{ kK}.$$

The above regression line is plotted in Fig. 9. It has a slope close to unity with

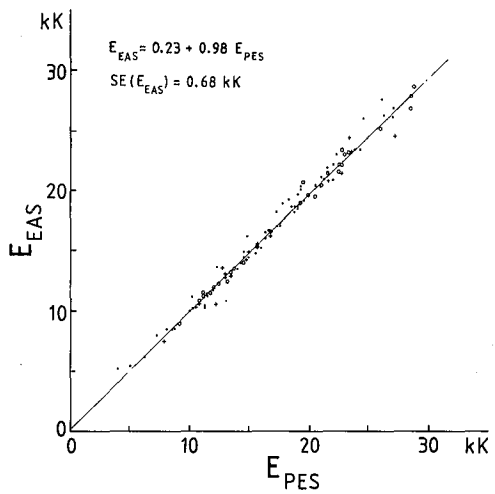

Fig. 9. Correlation diagram for energies of "*I*" type electronic transitions for condensed aromatic radical cations obtained from electronic absorption spectra (EAS) and photoelectron spectra (PES): catacondensed aromatics (•); perylenes and coronenes (+); pyrenes (o).

a small intercept which shows that (i) the matrix shift on moving from the solid phase (EA spectra) to the gas phase (PE spectra) is negligibly small and (ii) there is no significant change in the geometry of the molecules on their ionization. Furthermore, the smallness of the standard error clearly demonstrates that the overall correspondence between the two types of spectroscopies is excellent.

5. Concluding remarks

This paper completes our study of the correlation between optical absorption and photoelectron spectroscopies for condensed-ring aromatic hydrocarbon radical cations. It has once again been demonstrated that the PE spectroscopy provides a very useful technique, apart from open-shell SCF-CI methods, for characterizing electronic spectra of ion-radicals. On the basis of this study, it has been possible to rectify some of the earlier assignments of the ionic spectra.

Acknowledgments

The author is grateful to Prof. J. Wasilewski of the Department of Physics, Nicolas Copernicus University, Poland, for sending a corrected version of his paper and for very fruitful discussions through correspondence. Thanks are also due to Prof. Bashiruddin Ahmed, vice-chancellor, Jamia Millia Islamia, for granting financial support for the publication of this work.

References

[1] Z.H. Khan, *Z. Nat.forsch. A* **39**, 668 (1984); ibid. **42**, 91 (1987).

[2] Z.H. Khan, *Spectrochim. Acta A* **44**, 313 (1988); ibid. **45**, 253 (1989).

[3] W. Schmidt, *J. Chem. Phys.* **60**, 4406 (1974); ibid. **66**, 828 (1977).

[4] Z.H. Khan, *Can. J. Spectrosc.* **23**, 8 (1978).

[5] Z.H. Zaidi, B.N. Khanna, *J. Chem. Phys.* **50**, 3291 (1969); *Indian J. Pure Appl. Phys.* **7**, 753 (1969); ibid. **9**, 44 (1971).

[6] H.C. Longuet-Higgins, J.A. Pople, *Proc. R. Soc. Lond. A* **68**, 591 (1955).

[7] J. Wasilewski, *Acta Phys. Pol. A* **38**, 349 (1970).

[8] C.C.J. Roothaan, *Rev. Mod. Phys.* **32**, 179 (1960).

[9] Z.H. Khan, *Spectrochim. Acta A* **44**, 1125 (1988).

[10] R. Zahradnik, P. Carsky, *J. Phys. Chem.* **74**, 1235 (1970).

[11] J. Wasilewski, private communications. Also see Z.H. Khan, *Int. J. Quantum Chem.* **42**, 1717 (1992).

[12] R. Pariser, R.G. Parr, *J. Chem. Phys.* **21**, 466, 767 (1953).

[13] N. Mataga, K. Nishimoto, *Z. Phys. Chem. Frankfurt (Main)* **13**, 140 (1957).

[14] T. Shida, S. Iwata, *J. Am. Chem. Soc.* **95**, 3473 (1973).

[15] L. Andrews, R.S. Friedman, B.J. Kelsall, *J. Phys. Chem.* **89**, 4550 (1985).

[16] F. Salama, L.J. Allamandola, *J. Chem. Phys.* **94**, 6964 (1991).

[17] M.J.S. Dewar, S.D. Worley, *J. Chem. Phys.* **51**, 263 (1969).

[18] H. Hiratsuka, Y. Tanizaki, *J. Phys. Chem.* **83**, 2501 (1979).

[19] J. Spanget-Larsen, *Croat. Chem. Acta* **57**, 991 (1984).

[20] T. Bally, *Radical Ionic Systems*, Eds. A. Lund, M. Shiotani, Kluwer Academic Publishers, Dordrecht 1991, p. 14.

[21] Z.H. Khan, B.N. Khanna, *Z. Nat.forsch. A* **32**, 796 (1977).